Quinacrine and Ethidium Bromide Bind the Same Locus on the Nicotinic Acetylcholine Receptor from *Torpedo californica*†

Monica M. Lurtz, Michele L. Hareland,‡ and Steen E. Pedersen*

Department of Molecular Physiology and Biophysics, Baylor College of Medicine, Houston, Texas 77030

Received October 10, 1996; Revised Manuscript Received December 12, 1996⊗

ABSTRACT: Quinacrine is a noncompetitive antagonist of the nicotinic acetylcholine receptor (AChR) which displays severalfold fluorescent enhancement upon binding to AChR-rich membranes from *Torpedo californica* electric organ. It is demonstrated that the fluorescence enhancement comprises two components: specific interaction at a high-affinity binding site on the AChR, and interaction with the lipid bilayer. The interaction with the lipid bilayer can be attenuated by other noncompetitive antagonists, but at concentrations substantially higher than those required for binding to the AChR. It is further shown that quinacrine can inhibit the binding of [^{3}H]phencyclidine and [^{3}H]ethidium in a manner fully consistent with simple competitive inhibition. The data support a model for high-affinity quinacrine binding to the same, single locus of the acetylcholine receptor as phencyclidine and ethidium. This site is likely within the lumen of the ion channel.

The nicotinic acetylcholine receptor (AChR)[1] is a pentameric nonspecific cation channel composed of four nonidentical, homologous subunits with the stoichiometry of $\alpha_2\beta\gamma\delta$. Each of the five subunits possesses four putative transmembrane spanning sequences, termed M1, M2, M3, and M4. The amino termini form a large extracellular vestibular structure which includes the two acetylcholine binding sites [see Lena and Changeux (1993) for a review]. The narrow portion of the channel pore is lined by the five M2 domains, one from each subunit (Unwin, 1993; Imoto *et al.*, 1986; Giraudat *et al.*, 1987).

Noncompetitive antagonists (NCAs) block AChR action by binding to a site or sites distinct from the acetylcholine binding sites. Two classes of binding sites have been described: a high-affinity site that appears to bind with a stoichiometry of 1 per AChR (Krodel *et al.*, 1979; Heidmann *et al.*, 1983; Dreyer *et al.*, 1986; Giraudat *et al.*, 1987; Herz *et al.*, 1987) plus numerous low-affinity sites, perhaps as many as 30 per AChR (Heidmann *et al.*, 1983). Affinity labeling by reactive or photoreactive NCAs has provided insight on the location of the high-affinity NCA site. Chlorpromazine and triphenylmethylphosphonium specifically label residues within the M2 sequence at homologous sites on each of the subunits (Giraudat *et al.*, 1986, 1987, 1989; Hucho *et al*., 1986). Meproadifen mustard was localized to αGlu-262 in M2 on the α subunit (Pedersen *et al.*, 1992). Reactive sites for TID have been identified within the M2 sequence with the receptor stabilized in either the resting or the desensitized conformation (White & Cohen, 1992). Mutagenesis of residues within the M2 sequence also affects the affinity of open channel block by QX-222 (Charnet *et al.*, 1990).

Such data support a model of noncompetitive antagonism by steric occlusion of the ion pore itself. This model is further supported by the observations that the binding of many NCAs is also dependent upon receptor conformation. Phencyclidine (PCP), ethidium (EB), meproadifen, and quinacrine preferentially bind the desensitized state of the receptor, whereas tetracaine and TID preferentially bind the resting channel (Krodel *et al.*, 1979; Heidmann *et al.*, 1983; White *et al.*, 1991; Wu *et al.*, 1994). Nonetheless, it is possible that some NCAs act by allosteric mechanisms at sites distinct from the channel pore itself, and perhaps indirectly by perturbation of the lipid bilayer. Such mechanisms are difficult to exclude since many of the NCAs interact strongly with the bilayer as well (Krodel *et al.*, 1979).

Quinacrine is a strong membrane perturbant that is also an NCA. Quinacrine azide, a photoactivatable analog of quinacrine, reacts with the amino-terminal end of the putative M1 segment of the α subunit, a pattern distinct from any other characterized NCA affinity label (Dipaola *et al.*, 1990; Karlin, 1991). This compound was shown to react within 50 ms of exposure to agonist, consistent with labeling the open channel (Dipaola *et al.*, 1990). In contrast to the M2 domain that is thought to line the ion channel, the disposition of the putative transmembrane sequence M1 is less certain. Recent experiments tested the accessibility of cysteines substituted for residues in the N-terminal portion of the M1 sequence. Reaction of several such residues with polar modifying reagents resulted in partial channel blockade (Akabas & Karlin, 1995). The data suggest that this portion of M1 is also associated with the pore of the channel. This would support the model of quinacrine acting as do other NCAs, by sterically occluding the pore. However, it should be noted that mutations outside the ion channel may also affect channel conductivity and gating [*e.g.*, see Lee *et al.* (1994)].

† This work was supported by U.S. Public Health Service Grants NS28879 and NS35212. S.E.P. was supported by Research Career Development Award NS01618, M.M.L. was supported by Public Health Training Grant HL07676, and M.L.H. was supported by NSF Grant BIR-9322251.

* To whom correspondence should be addressed.

‡ Current address: Department of Chemical Engineering, California Institute of Technology, Pasadena, CA 91125.

⊗ Abstract published in *Advance ACS Abstracts,* February 1, 1997.

[1] Abbreviations: AChR, nicotinic acetylcholine receptor; ACh, acetylcholine; NCA, noncompetitive antagonist; EB, ethidium; PCP, phencyclidine; TFA, trifluoroacetic acid; TID, 3-(trifluoromethyl)-*m*-[^{125}I]iodophenyldiazirine.

S0006-2960(96)02547-0 CCC: $14.00

In support of a distinct allosteric model of noncompetitive antagonism, data have accrued that suggest the principal site of quinacrine binding is located at the protein−lipid interface of the AChR, near the outer leaflet of the bilayer (Valenzuela *et al.*, 1992; Arias *et al.*, 1993a). Fluorescence studies that compared quenching of quinacrine fluorescence to quenching of EB fluorescence by lipid-soluble spin-label quenchers showed substantially higher quenching of quinacrine than EB. Whereas the quenching of EB fluorescence was consistent with a luminal, ion channel binding site that was shielded from quenchers, the quenching of quinacrine fluorescence was consistent with a site more exposed to the lipid bilayer. It was proposed that binding to this site would inhibit channel opening and inhibit binding to the luminal NCA site allosterically, and preferentially bind the agonist-induced desensitized conformation (Valenzuela *et al.*, 1992; Arias *et al.*, 1993b; Arias & Johnson, 1995).

In this paper, we provide evidence by both fluorescence spectroscopy and radioligand binding assays that supports binding of quinacrine and EB to a single locus. It is shown that a substantial component of quinacrine fluorescence is due to interactions with the lipid bilayer and that this component is inhibitable by high concentrations of NCAs, even in the complete absence of AChR. We conclude that this fluorescence component may account for the quinacrine quenching data; moreover, the direct binding data support binding of EB and quinacrine at a common site.

EXPERIMENTAL PROCEDURES

Materials. Quinacrine dihydrochloride, ethidium bromide (EB), carbamylcholine chloride, phencyclidine hydrochloride (PCP), and 2-α-phosphatidylcholine type II-S (soy lipid) were purchased from Sigma Chemical Co. (St. Louis, MO). Ethidium bromide was crystallized from methanol prior to use. [^{3}H]PCP (43 Ci/mmol) was obtained from New England Nuclear. Proadifen, from Research Biochemicals International (Natick, MA), was used to synthesize meproadifen (Pedersen, 1995; Krodel *et al.*, 1979). HPLC grade methanol and acetonitrile were from Baker. Chloroform and trifluoroacetic acid (TFA) were HPLC grade from Fisher Scientific (Houston, TX) and Pierce (Rockford, IL), respectively. α-Bungarotoxin was purchased from Molecular Probes (Eugene, OR). Reactions were carried out either in 10 or 20 mM Hepes, pH 7.0, in 10 mM sodium phosphate, pH 7.4, or in HTPS (250 mM NaCl, 5 mM KCl, 3 mM $CaCl_2$, 2 mM $MgCl_2$, and 20 mM Hepes, pH 7.0).

Ethidium bromide (EB) was radiolabeled by catalytic exchange with ^3H_2O (25 mg of EB in 1 mL of dimethyl formamide, 0.5% TFA, and 25 mg of Rh/Al_2O_3 catalyst; carried out by Dupont/New England Nuclear). [^{3}H]EB was purified by cation exchange chromatography over CM-25 Sephadex (3 mL) and then by C-18 Sep-Pak (Millipore/Waters) chromatography. The [^{3}H]EB had greater than 90% radiochemical purity as assessed by reversed phase HPLC. The specific activity was 1.15 Ci/mmol. This was isotopically diluted to 0.21 Ci/mmol for ligand binding assays.

AChR-rich membranes were prepared from frozen *Torpedo californica* electric organ (Marinus, Long Beach, CA) by differential sucrose ultracentrifugation as previously described (Pedersen *et al.*, 1986). Typical membrane specific activity was 1.0−1.5 nmol of acetylcholine binding sites/mg of protein, as determined by [^{3}H]acetylcholine binding.

Torpedo Lipid Preparation and Reconstitution of Torpedo and Soy Lipids. *Torpedo* lipids were extracted from AChR-rich membranes essentially as described by Bligh and Dyer (1959) with the following modifications. The membranes were sedimented in a Beckman ultracentrifuge at 42 krpm for 30 min at 2 °C in a type 45 rotor. The membranes were resuspended in water, mixed with methanol and chloroform (0.8:2:1), and homogenized 2× with a Kontes Duall tissue grinder and transferred to a separatory funnel. Equal volumes of chloroform and water were then added to a final ratio of 0.9:1:1(water/methanol/chloroform). After separation, the organic (lower) layer was removed and reextracted with 1.9 volumes of an equivalent upper phase of methanol/water. The organic layer was concentrated by rotary evaporation, and the lipids were resuspended in chloroform and stored at −20 °C under argon. *Torpedo* lipids and soy lipids were reconstituted as needed in 10 mM phosphate buffer, pH 7.4, to 5 or 10 mg/mL by bath sonification to clarity before each use. For extracted lipid, the chloroform was evaporated from the lipid under a stream of argon, and dried under vacuum before reconstitution.

Radioligand Binding Assays. AChR-rich membranes were incubated for 1 h at ambient temperature in the presence of [^{3}H]PCP or [^{3}H]ethidium, plus inhibitor as indicated. Carbamylcholine was included in most experiments to promote desensitization of the AChR. After incubation, membranes were centrifuged at 18500*g* for 30 min at 20 °C in a TOMY MTX-150 centrifuge. To determine the free radioligand concentration, an aliquot of each supernatant was counted. Bound radioligand concentration was determined by counting the pellets after dissolving in 10% SDS. Meproadifen, PCP, or α-bungarotoxin was used to define nonspecific binding.

For binding isotherms, specific binding was determined by subtracting nonspecific from total binding. For determination of dissociation constants, specific binding data were fitted by a nonlinear least-squares algorithm (SigmaPlot version 2.0, Jandel Inc.) to eq 1: $B = L/(L + K_D)$, where B is the specific bound concentration, L the free ligand concentration, and K_D the corresponding dissociation constant. For inhibition experiments, determination of inhibition constants was accomplished by fitting data to a single inhibition site with eq 2: $B = B_{max}/(1 + I/K_{app}) + Bcg$, where B_{max} represents the specific binding in the absence of inhibitor, K_{app} represents the inhibitor concentration required for 50% inhibition, and Bcg represents the background binding (nonspecific binding). Because [^{3}H]PCP binding assays were routinely carried out at low concentrations (near 1 nM), well below the dissociation constant, the K_{app} is equal to the K_D for the competing ligand. For inhibition of [^{3}H]-EB binding, the equilibrium dissociation constants for the competing ligands, K_D, were calculated from the K_{app}s using eq 3: $K_D = K_{app}K_{EB}/(K_{EB} + L)$ where K_{EB} is the independently determined dissociation constant for [^{3}H]EB and L the free [^{3}H]EB concentration.

Fluorescence Spectroscopy. Fluorescence data were collected on an SLM 8000 fluorometer equipped with a 350 W xenon short arc lamp. Binding isotherms of [^{3}H]EB were conducted in 3 × 3 mm cuvettes; all other experiments were conducted in 10 × 10 mm cuvettes. For equilibrium binding measurements by EB fluorescence, the excitation wavelength was 340 nm, and the emission wavelength was 595 nm (4 and 16 nm bandwidths respectively). A visible absorbing filter (Oriel 59152) was used in the excitation path, and a 540 nm cut-on filter (Oriel 59502) was used in the emission

path. Free [^{3}H]EB concentrations were determined by counting the supernatant after centrifugation.

The dissociation kinetics of EB from the AChR were determined by continuous monitoring of fluorescence after addition of an inhibitor. To minimize interference from quinacrine fluorescence, the excitation and emission wavelengths were changed to 497 nm and 590 nm, respectively, with a 430 nm cut-on long-pass filter (Oriel 59480) in the excitation path and a 540 nm cut-on long-pass filter (Oriel 59502) in the emission path. Rates were determined for the data by fitting to a double-exponential decay described by eq 4: $F = A_1e^{-tk_1} + A_2e^{-tk_2} + \text{Bcg}$, where A_1 and A_2 are the amplitudes of each component, k_1 and k_2 are the corresponding rates (s^{-1}), and Bcg is the background fluorescence.

Quinacrine fluorescence excitation spectra were conducted in 10 mM phosphate buffer, pH 7.4, with 350 nM quinacrine, and in the presence of AChR-rich membranes (740 nM ACh binding sites) or *Torpedo* or soy lipid (0.75 mg/mL), with 1 mM carbamylcholine and varying concentrations of PCP. Excitation from 260−484 nm was monitored at an emission wavelength of 502 nm, with a 430 nm cut-on filter (Oriel 59480) in the emission path. Inhibition of quinacrine fluorescence by titration with PCP or other reagents was conducted by excitation at 450 nm and emission at 502 nm with 4 and 16 nm bandwidths, with a 430 nm cut-on filter (Oriel 59480) in the emission path.

Determination of Partition Coefficients. To determine the partition coefficient for quinacrine in either HTPS or 20 mM Hepes, AChR-rich membranes (350 nM receptor) were incubated for 1 h at ambient temperature in the presence of 1 mM carbamylcholine, 0.5 μM quinacrine, and 0, 10, or 500 μM PCP. After incubation, membranes were centrifuged at 18500*g* for 30 min at 20 °C in a TOMY MTX-150 centrifuge. Aliquots of supernatant were transferred to microfuge tubes containing 0.1% TFA (v/v), and the quinacrine concentration was then determined by HPLC. The membrane pellet was resuspended in 10 μL of buffer using a 50 μL Hamilton syringe and then transferred to microfuge tubes containing 190 μL of 0.1% TFA with 1 mM PCP and 0.1 M NaCl. The membranes were recentrifuged and the supernatants assayed by HPLC for quinacrine. Quinacrine concentrations were measured by HPLC on a C18 ultrasphere column (250 × 4.6 mm; Beckman Instruments) by comparison to a standard curve. HPLC was performed using a Beckman 125 System Gold, a Model 166 variable-wavelength detector (280 nm detection was used routinely), and data collection with System Gold software.

The partition coefficient was calculated from the quinacrine concentration in the pellet divided by the supernatant concentration. This value was then divided by the membrane protein concentration. The values, therefore, have the units of $(\text{mg/mL})^{-1}$. The partition coefficients for [^{3}H]EB and [^{3}H]-PCP were determined from various binding experiments in the presence of excess unlabeled noncompetitive antagonist from the counts in the pellets and supernatants and the protein concentration.

Ancillary Methods. Protein was measured using a bicinchoninic assay (Pierce, BCA microassay) with BSA as the standard protein. Mass spectroscopy for optimization of catalytic exchange conditions for ethidium bromide was carried out at the Baylor Mass Spectroscopy Core facility. [^{3}H]Acetylcholine binding to quantify the specific activity of AChR-rich membranes was performed as described previously (Pedersen, 1995).

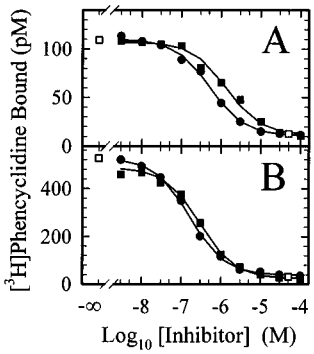

FIGURE 1: Ethidium and quinacrine inhibit [^{3}H]phencyclidine binding. AChR-rich membranes (50 μg; 62.5 nM AChR) were incubated for 1 h at ambient temperature in 400 μL of HTPS (panel A) or 20 mM Hepes (panel B) with 1 nM [^{3}H]PCP in the presence of 1 mM carbamylcholine and the indicated concentrations of EB (●), quinacrine (■), or meproadifen (□). Bound [^{3}H]PCP was determined as described under Experimental Procedures, and the data were fit to eq 2 (solid lines). Each symbol represents the average of duplicate determinations. The K_{app}s observed for EB and quinacrine, respectively, were 510 nM and 1.33 μM for HTPS, and 165 nM and 300 nM for Hepes.

RESULTS

To evaluate whether the fluorescent noncompetitive antagonists quinacrine and EB bind the same site or different sites on the AChR, we attempted to determine if the binding was mutually competitive, as would be consistent with binding to a single site, or whether the inhibition was allosteric, as would be consistent with distinct sites. Because of the inherent difficulties in using fluorescence spectroscopy to measure ligand binding over broad concentration ranges in the presence of substantial concentrations of two fluorescent species, we chose to initially examine their binding using radioligand binding assays. Inhibition assays using [^{3}H]PCP and [^{3}H]EB were used to characterize the binding of quinacrine to the NCA site. Conditions of both low ionic strength and physiological ionic strength are examined for comparison with quinacrine fluorescence data collected primarily in low ionic strength buffer.

Inhibition of [^{3}H]Phencyclidine Binding. Inhibition of [^{3}H]PCP binding by quinacrine and by EB was performed with a centrifugation assay using low concentrations (∼1 nM) of [^{3}H]PCP either in physiological saline (HTPS; Figure 1A) or in a low ionic strength buffer (20 mM Hepes, Figure 1B). Experiments included carbamylcholine to induce the desensitized conformation of the AChR. In either buffer, [^{3}H]PCP binding was inhibited by quinacrine or by EB to the same extent as by 50 μM meproadifen. In each case, the displacement is well characterized by a model for single site inhibition (solid lines). The salts included in the physiological buffer (HTPS) change the K_{app}s 2−4 fold, the effect being more pronounced for quinacrine. The higher binding observed in the low ionic strength buffer (Figure 1A *versus* 1B) also reflects a higher [^{3}H]PCP affinity in the low ionic strength buffer. The results demonstrate that both EB and quinacrine fully inhibit [^{3}H]PCP binding to the desensitized form of the AChR in a manner consistent with simple competitive binding. The average K_Ds for inhibition from this and similar experiments are given in Table 1.

Direct Binding of [^{3}H]Ethidium. Ethidium binding has been characterized by measuring the fluorescence enhancement upon binding the AChR (Herz *et al.*, 1987). In order to directly examine the binding of EB and to obviate concerns

Table 1: Dissociation Constants for Noncompetitive Antagonists in Low and High Ionic Strength Buffers[a]

NCA	assay	K_D (nM) Hepes	K_D (nM) HTPS
ethidium	fluorescence[b]	54 ± 13 (5)	795 ± 83 (2)
	[^{3}H]EB[c]	75 ± 22 (4)	575 ± 23 (2)
	[^{3}H]PCP[d]	200 ± 60 (2)	500 ± 120 (3)
meproadifen	[^{3}H]EB[e]	130 ± 50 (4)	400 ± 40 (2)
quinacrine	[^{3}H]EB[e]	260 ± 100 (7)	3000 ± 850 (2)
	[^{3}H]PCP[d]	288 ± 13 (2)	1300 ± 20 (2)
phencyclidine	[^{3}H]EB[e]	180 ± 60 (5)	450 ± 220 (2)
	[^{3}H]PCP[d]	95 ± 30 (5)	290 ± 190 (2)

[a] Hepes = low ionic strength buffer (10 or 20 mM Hepes); HTPS = *Torpedo* physiological saline buffer, as described under Experimental Procedures. Values represent the average of the number of discrete experiments (parentheses), and the errors are the standard deviation or the range (for values with only two determinations). [b] Dissociation constants were determined by fluorescence enhancement as described in Figure 2 and under Experimental Procedures. [c] Dissociation constants were determined from the counting data as described for Figure 2. [d] Dissociation constants for ethidium, quinacrine, and PCP were determined by the inhibition of [^{3}H]PCP binding as described for Figure 1. [e] Dissociation constants were calculated from the K_{app} for inhibition, the K_D for [^{3}H]EB, and the measured free [^{3}H]EB concentration, using eq 3 as described under Experimental Procedures.

about interference with the fluorescent signal by other ligands, [^{3}H]EB was synthesized from EB by catalytic exchange with tritiated water. The purity and specific radioactivity of the tritiated product were established by HPLC (see Experimental Procedures). Because both fluorescent spectroscopic assays and centrifugation assays were being used to characterize the binding to the NCA site, we determined whether the two assays were capable of producing comparable dissociation constants for [^{3}H]EB binding. As shown in Figure 2, [^{3}H]EB binding data to the AChR measured either by fluorescence enhancement (Figure 2A,B) or by counting radioactivity (Figure 2C,D) were saturable and were well described by single site binding functions (solid lines). The determinations were made in both physiological buffer (HTPS, Figure 2A,C) and low ionic strength buffer (Figure 2B,D).

In either buffer, a close correspondence between the K_Ds measured either by fluorescence or by counting [^{3}H]EB was observed (see Table 1 for a summary of the K_Ds). [^{3}H]EB binds with 10−15-fold higher affinity in low ionic strength (K_D = 50 nM) than in physiological buffer (K_D = 700 nM). The latter value is reasonably consistent with previous observations (Herz *et al.*, 1987) that were carried out at somewhat lower ionic strength. However, the K_D for binding in low ionic strength buffer differs substantially from the value determined by inhibition of [^{3}H]PCP binding. This is likely due to the significant nonspecific binding of EB that will create a substantial discrepancy between the total EB concentration and the actual free EB concentration. The nonspecific component of binding was linear in physiological buffer, as observed both by fluorescence and by radioactivity, but, for the low ionic strength buffer, the nonspecific component was nonlinear with free [^{3}H]EB concentration. The nonspecific component was higher for the radioactive determination (Figure 2D), suggesting that EB that interacts nonspecifically with membranes has a lower fluorescent yield than EB bound to the NCA site. In both low and high ionic strength, the data are fully consistent with the presence of a single high-affinity binding site. The fluorescent determination accurately reflects binding as measured by direct counting of [^{3}H]EB.

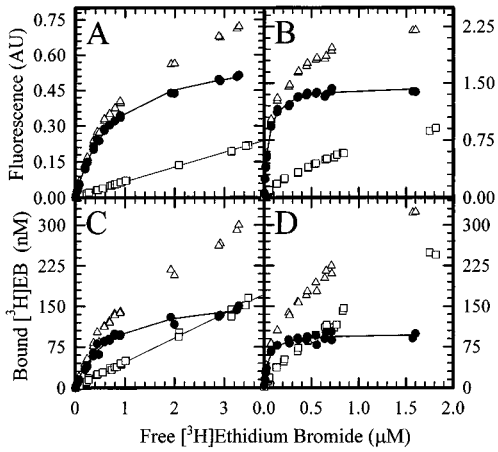

FIGURE 2: [^{3}H]EB binding to AChR by fluorescence assay and by centrifugation binding assays. AChR-rich membranes were incubated in either HTPS (A and C) or 20 mM Hepes buffer (B and D) with 1 mM carbamylcholine and varying concentrations of [^{3}H]-EB as described under Experimental Procedures. Panels A and B are fluorescence data for binding in HTPS (200 μL; 87 μg of AChR-rich membranes; 325 nM AChR) and in 20 mM Hepes (400 μL; 50 μg of AChR-rich membranes; 125 nM AChR), respectively. The fluorescence intensity for each sample was measured as described under Experimental Procedures. The corresponding binding data for the same samples were also determined by counting bound [^{3}H]-EB (panels C and D: HTPS and Hepes, respectively). For each set of data, specific binding (●) was determined by subtracting nonspecific (□) from total (△) binding. Nonspecific binding was determined in the presence of 100 μM PCP (for HTPS) or 50 μM PCP (Hepes); in the cases where the free [^{3}H]EB concentrations changed substantially with inclusion of PCP, the nonspecific binding was determined by interpolation (for the Hepes samples) or from the linear fit to the nonspecific component (for the HTPS samples; solid lines). Solid curves represent the best fit to a single-site equation (see Experimental Procedures). The K_Ds determined from the fits for this experiment were as follows: in HTPS, 740 nM by fluorescence and 590 nM by [^{3}H]EB; in Hepes, 45 nM by fluorescence and 44 nM by [^{3}H]EB.

Inhibition of [^{3}H]Ethidium Binding. [^{3}H]EB binding was inhibited by quinacrine, PCP, or meproadifen as determined using the centrifugation assay (Figure 3). In HTPS buffer, [^{3}H]EB binding was inhibited completely, and the data were well fit by a binding function for single-site inhibition (Figure 3A, solid lines). Similar curves for PCP inhibition were also obtained using fluorescence spectroscopy [data not shown; see also Herz *et al.* (1987)]. α-Bungarotoxin also inhibits EB binding (Herz *et al.*, 1987), and therefore control samples containing α-bungarotoxin were also included to help define nonspecific binding (▽). Figure 3B depicts results from a similar set of experiments conducted in low ionic strength buffer (20 mM Hepes). The inhibition by meproadifen, PCP, and α-bungarotoxin reaches similar levels at high concentrations and defines a level of substantial nonspecific binding (consistent with the data in Figure 2) that was approximately half of the total observed binding. Remarkably, moderate concentrations (∼1 μM) of quinacrine decreased [^{3}H]EB binding to substantially lower levels than those defined by α-bungarotoxin, PCP, or meproadifen. Furthermore, these data were also well described by a single-site binding equation (solid lines). This suggests either the existence of a second binding site that is inhibitable by quinacrine but not by the other antagonists or, more likely, the existence of potent membrane interactions of quinacrine that affect the nonspecific binding of [^{3}H]EB.

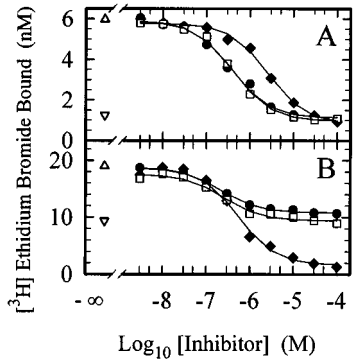

FIGURE 3: Phencyclidine, quinacrine, and meproadifen inhibit [^{3}H]-ethidium binding. AChR-rich membranes (100 μg; 67 nM AChR) were incubated in 1 mL of buffer, [^{3}H]EB, 1 mM carbamylcholine, and the indicated concentrations of PCP (●), meproadifen (□), and quinacrine (◆). Data are also shown for carbamylcholine only (△) and for 420 nM α-bungarotoxin (▽). Panel A: HTPS buffer with 55 nM [^{3}H]EB. Panel B: 20 mM Hepes buffer with 40 nM [^{3}H]-EB. Solid lines represent the best fits to single-site inhibition curves. Each symbol represents the average of duplicate determinations. The K_{app}s determined from the fitted parameters were as follows for HTPS and Hepes, respectively: PCP, 313 and 215 nM; quinacrine, 2.57 μM and 542 nM; meproadifen, 410 and 251 nM.

The equilibrium dissociation constants (K_Ds) for each compound were calculated from the K_{app}s for inhibition and the K_D for EB using eq 3 and are listed in Table 1. The K_D values for quinacrine were consistent whether measured by inhibition of [^{3}H]EB binding or [^{3}H]PCP binding (Table 1). The value for the inhibition in low ionic strength must be considered in view of the apparent effects of quinacrine on nonspecific binding as well; that value is poorly determined by this assay. Nonetheless, the data of these experiments are fully consistent with simple, mutually competitive interactions of quinacrine with PCP and with EB at the high-affinity NCA site.

Quinacrine-Induced Ethidium Dissociation. The data of Figure 3 demonstrate complete inhibition of EB binding by quinacrine, consistent with simple competitive inhibition at a single site. However, strong allosteric coupling from binding to a distinct site could have produced similar results. A consequence of allosteric inhibition of ligand binding is a change in the association rate constant, the dissociation rate constant, or in both, whereas no change in the dissociation rate is predicted for a simple competitive mechanism. Thus, if quinacrine acts to lower the affinity of EB allosterically, a change in the rate constants for binding is predicted.

The rate of dissociation of EB from the AChR was measured by its concomitant fluorescence decrease after addition of inhibitors. As shown in Figure 4, fluorescence was monitored with time after addition of 40 μM inhibitor, either quinacrine (upper trace) or PCP (lower trace). The data were fit to a biexponential decay (eq 4). The two rate constants were similar for the two ligands (Table 2) and to those observed by Herz *et al.* (1991) for dissociation induced either by PCP or by various cations. The initial rapid increase in signal in trace 1 (Figure 4) is due to quinacrine fluorescence. This was verified by subsequent addition of quinacrine to the PCP sample after the PCP-induced changes were complete. This resulted in an increase in the background signal to the level of the quinacrine sample; conversely, addition of an equivalent concentration of PCP to the quinacrine sample did not result in a further change in the signal (data not shown). The data demonstrate that

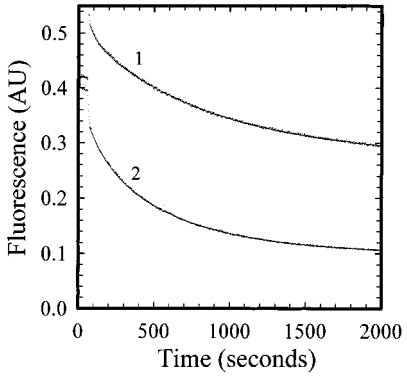

FIGURE 4: Ethidium dissociation induced by phencyclidine or quinacrine. AChR-rich membranes (100 nM AChR) were incubated in 1.75 mL of HTPS, 100 nM EB, and 1 mM carbamylcholine. The changes in EB fluorescence were measured upon addition of 40 μM quinacrine (trace 1) or PCP (trace 2) by monitoring the fluorescence decay on an SLM 8000 fluorometer (excitation, 497 nm; emission, 590 nm). The solid lines represent the best fit to a double-exponential decay (see Experimental Procedures).

Table 2: Rate Constants for Ethidium Dissociation Induced by Quinacrine or by Phencyclidine[a]

	A_1	k_1 (s^{-1})	A_2	k_2 (s^{-1})
quinacrine	0.106	0.0175	0.231	0.00122
phencyclidine	0.0956	0.00826	0.201	0.00173

[a] Values are from the nonlinear least-squares fitting of the data, shown in Figure 4, to eq 4, given under Experimental Procedures. A_1 and A_2 are the amplitudes of the fast and slow components, respectively, in arbitrary units of fluorescence; k_1 and k_2 are the corresponding rates.

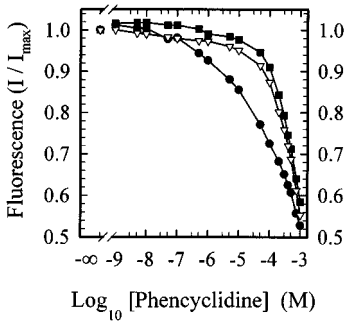

FIGURE 5: Inhibition of quinacrine fluorescence by phencyclidine is inconsistent with simple displacement of binding. PCP was titrated into cuvettes containing 350 nM quinacrine in 10 mM phosphate buffer, pH 7.4, with 1 mM carbamylcholine, and *Torpedo* AChR (0.75 mg/mL protein, ●), 0.75 mg/mL *Torpedo* extracted lipid (■), or 0.75 mg/mL soy lipid (▽). Quinacrine fluorescence was measured on an SLM 8000 fluorometer at each PCP concentration (excitation at 450 nm; emission at 502 nm). Each data set was normalized to its initial fluorescence value.

the dissociation rate of EB is independent of the competing ligand.

Phencyclidine Decreases Nonspecific Quinacrine Fluorescence. Quinacrine interaction with AChR-rich membranes is accompanied by increased fluorescence that is presumably due to binding to a high-affinity noncompetitive site. We initially examined inhibition of quinacrine binding by the nonfluorescent NCA PCP (Figure 5). In the presence of AChR-rich membranes suspended in a low ionic strength buffer, fluorescence was monotonically decreased by the sequential addition of PCP. Inhibition failed to approach a plateau value at concentrations up to 1 mM, and the distinctly nonsigmoidal curve could not be fit by a single binding site inhibition model. The concentration of quinacrine used in this experiment was near its K_D; therefore, the concentration

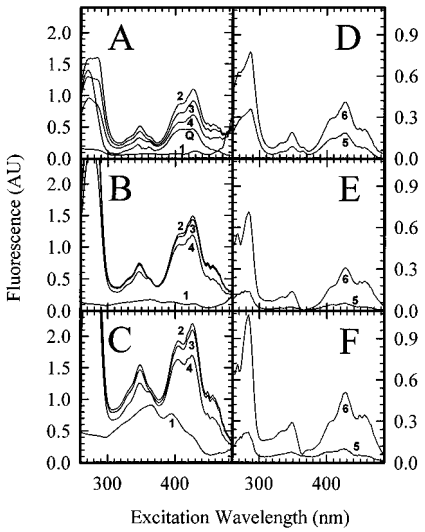

FIGURE 6: High PCP concentrations decrease quinacrine fluorescence in AChR-free lipid. Excitation spectra in 10 mM phosphate buffer, pH 7.4, in the presence of 1 mM carbamylcholine were taken on an SLM 8000 fluorometer, and emission was collected at 502 nm as described under Experimental Procedures. Panel A: 350 nM quinacrine (trace Q); *Torpedo* AChR (0.75 mg/mL protein) without quinacrine (trace 1); *Torpedo* AChR with 350 nM quinacrine (trace 2); *Torpedo* AChR with 350 nM quinacrine and 10 μM (trace 3) or 500 μM (trace 4) PCP. Panel B: *Torpedo*-extracted lipid (trace 1) and with the same additions as described for panel A (traces 2−4). Panel C: Soy lipid (trace 1) and with the same additions as described for panel A (traces 2−4). Panels D, E, and F: Difference spectra for *Torpedo* AChR, *Torpedo*-extracted lipid, or soy lipid, respectively, were obtained by subtraction of the corresponding excitation spectra shown in panels A, B, and C, and represent the magnitude of fluorescence decrease caused by 10 μM PCP (trace 5 = trace 2 − trace 3) and by 500 μM PCP (trace 6 = trace 2 − trace 4).

of PCP required for 50% inhibition (EC_{50}) should be near 1 μM. The EC_{50} in this experiment is near 100 μM, suggesting that PCP inhibition of quinacrine fluorescence does not occur solely by binding the NCA site of the AChR.

To examine whether PCP could affect quinacrine fluorescence in the absence of AChR, parallel titrations were carried out using lipids extracted from *Torpedo* AChR-rich membranes and using soy asolectin (Figure 5; ■ and ▽, respectively). Low concentrations of PCP (<10 μM) do not decrease quinacrine fluorescence. However, high concentrations of PCP (>100 μM) can clearly decrease quinacrine fluorescence in the presence of these lipids in the same manner observed for AChR-rich membranes. This suggests the presence of both AChR-specific and nonspecific components of fluorescence. Titration of the quinacrine fluorescence in the presence of AChR-rich membranes clearly shows a fluorescence decrease at concentrations of PCP expected to produce binding at the NCA site (0.5−10 μM), and this component was absent in the artificial liposomes. High concentrations of PCP can affect quinacrine fluorescence regardless of the presence of AChR.

Quinacrine Excitation Spectra. To further examine the influence of lipid interactions on quinacrine fluorescence, we compared quinacrine fluorescence excitation spectra in the presence of 0, 10, or 500 μM PCP for *Torpedo* membrane vesicles, for *Torpedo* lipids, and for soy lipid (Figure 6). The PCP concentrations were chosen either to inhibit >90% of the quinacrine binding to the high-affinity NCA site (10 μM) or to show effects both in the AChR-rich membranes and in the pure lipids (500 μM).

Table 3: Partition Coefficients for Ethidium, Phencyclidine, and Quinacrine in Low Ionic Strength Buffer and in Physiological Buffer[a]

	ethidium	phencyclidine	quinacrine
HTPS	0.17 ± 0.040, $n = 6$	0.051 ± 0.01, $n = 19$	0.133 ± 0.008, $n = 4$
Hepes	2.00 ± 0.27, $n = 10$	0.11 ± 0.02, $n = 24$	8.97 ± 0.21, $n = 4$

[a] Partition coefficients were calculated as described under Experimental Procedures and have units of $(mg/mL)^{-1}$. The errors are the standard deviations from n determinations.

The fluorescent excitation spectrum of quinacrine in the absence of membranes is shown in Figure 6A (*Q*) for reference. Interaction with AChR-rich membranes (Figure 6A, trace 2) produces an increase in fluorescence intensity: the increase is not merely due to the intrinsic fluorescence of the membranes alone (Figure 6A, trace 1). Addition of 10 μM PCP results in an appreciable decrease in fluorescence intensity in the presence of intact AChR; the difference is shown in Figure 6D, trace 5. After addition of 500 μM PCP, there is a further decrease in fluorescence intensity. The difference spectrum in Figure 6D, trace 6, shows the magnitude of the decrease.

In the absence of receptor, there was little decrease in the observed fluorescence intensity after addition of 10 μM PCP (compare traces 2 and 3; Figure 6B for *Torpedo* lipids, Figure 6C for soy lipids), but a substantial decrease upon addition of 500 μM PCP (compare traces 2 and 4 in Figure 6B,C). The difference spectra for 500 μM PCP were similar for all three types of membranes (traces 6 in Figure 6D,E,F). In contrast, 10 μM PCP produced a substantially larger decrease for AChR-rich membranes than for the artificial liposomes without AChR (compare trace 5 in Figure 6D to those in Figure 6E,F). The difference spectrum of binding to AChR-rich membranes (trace 5, Figure 6D) reflects predominantly specific binding of quinacrine to the AChR. The spectrum was of lower intensity, but qualitatively similar to the difference spectra produced by 500 μM PCP, therefore showing no particular changes in the excitation spectra whether quinacrine was bound to the AChR or interacting with the lipid bilayer. The data indicate the presence of at least two components of quinacrine fluorescence in the presence of AChR-rich membranes: one due to interaction with the high-affinity NCA site and a second due to interaction with the lipid bilayer. A number of control experiments established that PCP itself did not decrease quinacrine fluorescence in the absence of membranes nor by mechanisms such as inner filter effects.

Membrane Partitioning of Noncompetitive Antagonists. The increase in quinacrine fluorescence that was due to interaction with the lipid bilayer should be reflected by association of quinacrine with the membrane. Therefore, samples were centrifuged to collect the membranes, and quinacrine in both the supernatant and the pellet was quantified by HPLC. The determinations were made in both physiological buffer and low ionic strength buffer, and in the presence of 10 μM PCP to block binding to the NCA site. The ratio of sedimented quinacrine to free quinacrine was compared to ratios for EB and PCP, as measured by [^{3}H]EB and [^{3}H]PCP from various binding assays (Table 3). The data were normalized to the membrane protein concentration and therefore have the units of $(mg/mL)^{-1}$.

In physiological ionic strength, the interaction with the AChR-rich membranes differed only 3-fold for the three compounds, whereas striking differences were observed in

low ionic strength buffer. The interaction of PCP with the membrane increased only moderately in low ionic strength as compared with high ionic strength; however, EB and quinacrine interaction increased 12- and 70-fold, respectively. The large differences in partitioning correlate well to the difficulties in measuring the direct binding of these ligands in low ionic strength media. The difference between quinacrine and the other ligands is consistent with the fluorescence increase observed for quinacrine in the presence of AChR-free lipids. Thus, under the condition of binding assays in low ionic strength buffers, most of the quinacrine was associated with the lipid bilayer. Addition of 500 μM PCP reduced membrane partitioning of quinacrine to $\sim$4 $(mg/mL)^{-1}$ (data not shown), consistent with the decrease in fluorescence observed at the higher PCP concentrations. Thus, the fluorescence decrease caused by high concentrations of PCP was likely due to displacement of quinacrine from the membrane by PCP.

DISCUSSION

The interactions of EB and quinacrine with the nicotinic acetylcholine receptor were examined to determine whether they bind either the same or distinct loci on the protein. The inhibition of [^{3}H]PCP binding and of [^{3}H]EB binding by quinacrine was fully consistent with simple competitive inhibition both in physiological saline and in low ionic strength buffer. Inhibition of quinacrine fluorescence by PCP in low ionic strength buffer, however, was not saturable at high PCP concentrations. This observation was consistent with two components of quinacrine fluorescence: one that was inhibitable at low concentrations and dependent on the presence of the AChR and a second component that was inhibitable at high concentrations of PCP and was independent of the presence of AChR. The latter component could also be observed in artificial liposomes devoid of AChR. It is concluded that quinacrine binds to the high-affinity NCA site that is also bound by ethidium and PCP.

Quinacrine and Ethidium Binding. Synthesis of [^{3}H]EB permitted us to examine more directly the relationship between the binding of quinacrine and ethidium than possible by [^{3}H]PCP binding. The excellent agreement between fluorescence enhancement and the [^{3}H]EB binding demonstrates that fluorescence enhancement accurately reflects specific binding. The direct measurement of binding in low ionic strength also demonstrated a $\sim$10-fold increase in affinity for EB. This was less evident from the measurements of [^{3}H]PCP inhibition by EB that produced a higher K_D value (Table 1). This discrepancy was due to the interaction of EB with the membrane which causes the free concentration to be substantially lower than the total concentration in the sample. The K_Ds for ligands that interact strongly with the membrane are therefore significantly overestimated by competitive binding assays where the free competitor concentration is not determined explicitly. Thus, it its likely that the K_Ds for meproadifen and particularly for quinacrine are also overestimated in low ionic strength. This does not appear to be a problem for PCP, whose partitioning was less dependent on ionic strength.

To formally distinguish an allosteric mechanism of inhibition *versus* a competitive mechanism by equilibrium binding can be difficult because strong allosteric coupling may appear competitive. In physiological saline, inhibition of [^{3}H]EB by quinacrine, PCP, and meproadifen all approached the nonspecific level of binding, and the K_Ds derived from the K_{app}s are reasonably consistent with the values obtained by inhibition of [^{3}H]PCP binding (Table 1). This suggests that if allosteric mechanisms of inhibition were active, the coupling between the two sites must be greater than 10-fold, since residual binding would have been observed otherwise. Kinetic analysis should help distinguish competitive from allosteric mechanisms of inhibition, as allosteric mechanisms of inhibition must increase the dissociation rate, decrease the association rate, or both. However, for the AChR, the kinetics may be dominated by slow conformational changes that could obfuscate the interpretation of kinetic data. Nonetheless, it was shown that quinacrine does not accelerate the dissociation of EB from its binding site. EB dissociation was characterized by the similar rate constants whether quinacrine or PCP was the inhibiting ligand, and these constants agree well with those obtained by Herz *et al.* (1991).

The binding data suggest that the occupation of a high-affinity site for quinacrine results in displacement of both EB and PCP binding. Both the kinetics and equilibrium experiments were consistent with a competitive mechanism. Nonetheless, allosteric inhibition may not be distinguishable from competitive inhibition in this case; thus, our data do not prove, *sensu stricto*, that quinacrine and EB bind the same site. However, we did not observe any evidence in favor of allosteric inhibition. The ubiquitous presence of carbamylcholine in these experiments would strongly drive the desensitized conformation of the AChR; to propose the presence of further, distinct conformational changes to mediate allosteric inhibition of PCP or EB binding by quinacrine seems unwarranted without more evidence.

Quinacrine Interactions with the Membrane. Our radioligand binding data do not directly address the locus or loci of quinacrine binding except to suggest that quinacrine at least binds the same site occupied by EB and PCP. The strong interaction of quinacrine with the lipid bilayer in low ionic strength solutions suggests caution in interpretation of quinacrine fluorescence as a measure of high-affinity binding to the AChR. The data of Figures 5 and 6 and of Table 3 demonstrate that much of the fluorescence enhancement of quinacrine was due to interactions with the lipid bilayer and that pharmacological specificity of fluorescence cannot be demonstrated: PCP itself decreases quinacrine fluorescence through interactions in the membrane, independent of the presence of receptor. If high concentrations of PCP are used to define nonspecific binding, then the lipid interaction is suppressed and the *apparent* specific fluorescence comprises both high-affinity binding and lipid interaction. The lipid interaction component can be as much as 50% of the signal suppressible by 500 μM PCP in AChR-rich membranes (Figure 6D).

Evidence for the binding of quinacrine to the lipid−protein interface at a site distinct from that bound by EB was obtained from the differential fluorescence quenching by lipophilic spin-label reagents (Valenzuela *et al.*, 1992; Arias *et al.*, 1993a). EB was found to be less quenched than quinacrine, suggesting a more lipid-accessible site for quinacrine binding. These experiments were performed at low ionic strength and used high PCP concentrations (usually 500 μM) to define nonspecific binding. Our data suggest that a substantial proportion of the measured fluorescence difference was likely due to membrane interaction; this

fluorescence component would clearly be more accessible to the lipophilic spin-labels than a fluorophore bound to the lumen of the ion channel. In contrast, EB does not suffer from the same artifacts. Although EB also interacts strongly with the lipid bilayer in low ionic strength buffer, this effect is 4-fold less than for quinacrine (Table 3), and inhibition of [^{3}H]EB binding and fluorescence by PCP was well described by single-site inhibition curves (Figure 3B). Single-site inhibition curves were also obtained for radioligand assays performed at the higher membrane concentrations that were used to measure quinacrine fluorescence (data not shown). Thus, whereas PCP can properly define specific binding for EB fluorescence, it cannot do so for quinacrine. This difference in the membrane interactions of EB and quinacrine accounts for the differences in their quenching by spin-labeled lipids without invoking a lipid−interface binding site for quinacrine.

The NCA Binding Site Locus. Whereas the site of action of several NCAs has been localized to the M2 pore region by affinity labeling or by site-directed mutagensis, no comparable direct localization exists for phencyclidine or for ethidium. EB fluorescence was inhibited by cations with a rank order that reflects their conductance (Herz *et al.*, 1991), and EB was been shown to be an open channel blocker at the frog neuromuscular junction (Stertz *et al.*, 1982). Both experiments suggest that EB binds within the pore, comparable to other NCA ligands. Although fluorescence energy transfer measurements place EB in the large outer vestibule of the AChR, at a site distant from the narrow portion of the channel lumen (Johnson & Nuss, 1994), the 52 Å distance between EB and the extracellular lipid headgroups may also be consistent with a location within the narrow lumen of the channel, deeply below the plane of the lipid headgroups.

The size of the channel and the distant locations of reaction by chlorpromazine and meproadifen mustard leave the possibility that various ligands may bind preferentially to distinct regions of the channel. For instance, in the presence of agonist, TID can occupy the channel simultaneously with histrionicotoxin but fully competes with [^{3}H]phencyclidine (White *et al.*, 1991). Nonetheless, phencyclidine and histrionicotoxin bind in a competitive manner (Heidmann *et al.*, 1983). Repulsion may be mediated electrostatically *via* their positive charges, or by steric hindrance within the confines of the channel. TID, being both neutral and substantially smaller than other NCAs, may permit double occupancy with some NCAs and not others.

The mutually exclusive binding of ethidium and quinacrine likely reflects interaction at a single locus. Nonetheless, the data do not exclude binding to respective regions of the pore with partial overlap, or with repulsion through short-range electrostatic effects. This conclusion suggests that the residues tentatively identified as the reactive sites for quinacrine azide (αArg209 and αPro211; Karlin, 1991) are associated with the channel lumen rather than a lipid interface site, although labeling by quinacrine azide was carried out in a manner likely to promote reaction with the open channel rather than to the desensitized conformation. Recent data suggesting that the quinacrine locus is also the site for agonist self-inhibition (Arias & Johnson, 1995) are also consistent with quinacrine binding in the channel lumen as this is the likely locus for agonist-mediated open channel blockade (Forman & Miller, 1988, 1989a,b).

ACKNOWLEDGMENT

Arlene Samano is thanked for superb technical assistance in binding experiments.

REFERENCES

Akabas, M. H., & Karlin, A. (1995) *Biochemistry 34*, 12496−12500.
Arias, H. R., & Johnson, D. A. (1995) *Biochemistry 34*, 1589−1595.
Arias, H. R., Valenzuela, C. F., & Johnson, D. A. (1993a) *J. Biol. Chem. 268*, 6348−6355.
Arias, H. R., Valenzuela, C. F., & Johnson, D. A. (1993b) *Biochemistry 32*, 6237−6242.
Bligh, E. G., & Dyer, W. J. (1959) *Can. J. Biochem. Physiol. 37*, 911−917.
Charnet, P., Labarca, C., Leonard, R. J., Vogelaar, N. J., Czyzyk, L., Gouin, A., Davidson, N., & Lester, H. A. (1990) *Neuron* 2, 87−95.
DiPaola, M., Kao, P. N., & Karlin, A. (1990) *J. Biol. Chem. 265*, 11017−11029.
Dreyer, E. B., Hasan, F., Cohen, S. G., & Cohen, J. B. (1986) *J. Biol. Chem. 261*, 13727−13734.
Forman, S. A., & Miller, K. W. (1988) *Biophys. J. 54*, 149−158.
Forman, S. A., & Miller, K. W. (1989a) *Trends Pharmacol. Sci. 10*, 447−452.
Forman, S. A., & Miller, K. W. (1989b) *Biochemistry 28*, 1678−1685.
Giraudat, J., Dennis, M., Heidmann, T., Chang, J.-Y., & Changeux, J.-P. (1986) *Proc. Natl. Acad. Sci. U.S.A. 83*, 2719−2723.
Giraudat, J., Dennis, M., Heidmann, T., Haumont, P.-Y., Lederer, F., & Changeux, J.-P. (1987) *Biochemistry 26*, 2410−2418.
Giraudat, J., Galzi, J.-L., Revah, F., Changeux, J.-P., Haumont, P.-Y., & Lederer, F. (1989) *FEBS Lett. 253*, 190−198.
Heidmann, T., Oswald, R. E., & Changeux, J. P. (1983) *Biochemistry 22*, 3112−3127.
Herz, J. M., Johnson, D. A., & Taylor, P. (1987) *J. Biol. Chem. 262*, 7238−7247.
Herz, J. M., Kolb, S. J., Erlinger, T., & Schmid, E. (1991) *J. Biol. Chem. 266*, 16691−16698.
Hucho, F., Oberthür, W., & Lottspeich, F. (1986) *FEBS Lett. 205*, 137−142.
Imoto, K., Methfessel, C., Sakmann, B., Mishina, M., Mori, Y., Konno, T., Fukuda, K., Kurasaki, M., Bujo, H., Fujita, Y., & Numa, S. (1986) *Nature 324*, 670−674.
Johnson, D. A., & Nuss, J. M. (1994) *Biochemistry 33*, 9070−9077.
Karlin, A. (1991) *Harvey Lect. 85*, 71−107.
Krodel, E. K., Beckman, R. A., & Cohen, J. B. (1979) *Mol. Pharmacol. 15*, 294−312.
Lee, Y.-H., Li, L., Lasalde, J., Rojas, L., McNamee, M., Ortiz-Miranda, S. I., & Pappone, P. (1994) *Biophys. J. 66*, 646−653.
Lena, C., & Changeux, J.-P. (1993) *Trends Neurosci. 16*, 181−186.
Pedersen, S. E. (1995) *Mol. Pharmacol. 47*, 1−9.
Pedersen, S. E., Dreyer, E. B., & Cohen, J. B. (1986) *J. Biol. Chem. 261*, 13735−13743.
Pedersen, S. E., Sharp, S. D., Liu, W.-S., & Cohen, J. B. (1992) *J. Biol. Chem. 267*, 10489−10499.
Stertz, M. H., Peper, K., & Bradley, R. J. (1982) *Eur. J. Pharmacol. 80*, 393−399.
Unwin, N. (1993) *J. Mol. Biol. 229*, 1101−1124.
Valenzuela, C. F., Kerr, J. A., & Johnson, D. A. (1992) *J. Biol. Chem. 267*, 8238−8244.
White, B. H., & Cohen, J. B. (1992) *J. Biol. Chem. 267*, 15770−15783.
White, B. H., Howard, S., Cohen, S. G., & Cohen, J. B. (1991) *J. Biol. Chem. 266*, 21595−21607.
Wu, G., Raines, D. E., & Miller, K. W. (1994) *Biochemistry 33*, 15375−15381.

BI962547P